crystals

MDPI

Article

Rare-Earth Fluorite-like $Li_{0.42}La_{4.58}Mo_3O_{15.76\pm\delta}F_{0.42\pm\varepsilon}$ Molybdates: Crystal Growth and Atomic Structure

Ekaterina I. Orlova [1,2,*], Timofei A. Sorokin [2], Vladimir B. Kvartalov [2], Alexander M. Antipin [2], Nataliya E. Novikova [2,*], Elena P. Kharitonova [1,2], Nataliya I. Sorokina [2], Olga A. Alekseeva [2] and Valentina I. Voronkova [1]

[1] Faculty of Physics, Lomonosov Moscow State University, GSP-1, Leninskiye Gory, 119991 Moscow, Russia; harit@polly.phys.msu.ru (E.P.K.); voronk@polly.phys.msu.ru (V.I.V.)
[2] Shubnikov Institute of Crystallography of Federal Scientific Research Centre "Crystallography and Photonics" of Russian Academy of Sciences, Leninskiy Prospekt 59, 119333 Moscow, Russia; tim29@inbox.ru (T.A.S.); kvartalov@gmail.com (V.B.K.); antipin@physics.msu.ru (A.M.A.); nsor@ns.crys.ras.ru (N.I.S.); olalex@crys.ras.ru (O.A.A.)
* Correspondence: agapova@polly.phys.msu.ru (E.I.O.); nata110565@mail.ru (N.E.N.); Tel.: +7-495-939-28-83 (E.I.O.)

Abstract: Rare-earth fluorine-containing molybdates of the $Ln_5Mo_3O_{16+\delta}$ oxygen–electron conductor family with the $LiLa_4Mo_3O_{15}F$ composition were synthesized for the first time as single crystals by the flux method. An accurate X-ray diffraction analysis of the obtained crystals was carried out at 20 and −183 °C. The $LiLa_4Mo_3O_{15}F$ compound is isostructural to the fluorine-free analogue with a cubic structure (space group $Pn\bar{3}n$). It is shown that lithium atoms replace one of the two positions of lanthanum in the more distorted LaO_8 polyhedron. According to X-ray diffraction analysis, fluorine atoms replace the positions of over-stoichiometric oxygen located in the vast cavities of the structure. So, fluorine anions can promote the interstitial conductivity of F-containing $LiLa_4Mo_3O_{15}F$ molybdates.

Keywords: crystal growth; crystal structure; rare-earth molybdates; fluorine-containing molybdates; oxyfluorides; $Nd_5Mo_3O_{16}$; $LiLa_4Mo_3O_{15}F$

check for updates

Citation: Orlova, E.I.; Sorokin, T.A.; Kvartalov, V.B.; Antipin, A.M.; Novikova, N.E.; Kharitonova, E.P.; Sorokina, N.I.; Alekseeva, O.A.; Voronkova, V.I. Rare-Earth Fluorite-like $Li_{0.42}La_{4.58}Mo_3O_{15.76\pm\delta}F_{0.42\pm\varepsilon}$ Molybdates: Crystal Growth and Atomic Structure. *Crystals* **2023**, *13*, 1009. https://doi.org/10.3390/cryst13071009

Academic Editor: Paola Paoli

Received: 14 June 2023
Revised: 22 June 2023
Accepted: 23 June 2023
Published: 25 June 2023

Copyright: © 2023 by the authors. Licensee MDPI, Basel, Switzerland. This article is an open access article distributed under the terms and conditions of the Creative Commons Attribution (CC BY) license (https://creativecommons.org/licenses/by/4.0/).

1. Introduction

Cubic rare-earth molybdates with the $Ln_5Mo_3O_{16+\delta}$ (*Ln* = La–Gd) composition, or Hubert phases [1], are of interest as potential electrode materials for medium-temperature solid oxide fuel cells [2]. The mixed oxygen–electron conductivity of these compounds reaches 10^{-2} S cm^{-1} at 700 °C [2–5]. The cubic structure (space group $Pn\bar{3}n$) [6,7] of Hubert phases is a derivative of the CaF_2 structure and is made up of LnO_8 cubes and isolated distorted MoO_4 tetrahedra with the formation of octahedral cavities (interstices) that can contain over-stoichiometric oxygen. So, the general formula of the compounds can be written as $Ln_5Mo_3O_{16+\delta}$, where δ is the amount of additional oxygen that can be controlled by changing the synthesis atmosphere or temperature and can be varied from 0 to 0.5 [3]. The interstitial oxygen atoms in the structure make the main contribution to the anion conductivity of $Ln_5Mo_3O_{16+\delta}$ compounds.

The fluorite-like structure of the $Ln_5Mo_3O_{16+\delta}$ Hubert phases remains stable under heterovalent doping. The family of these compounds has been extended, for example, with $MeLn_4Mo_3O_{16}$ (*Me* = Pb, Cd, Ca, Sr) phases [8–10]. There are a number of works [11–14] in which the possibility of replacing molybdenum with other atoms—for example, tungsten, vanadium, or niobium—was studied. In some works [8,15–17], the effect of partial co-doping of Hubert phases with an alkali cation and fluorine was studied: compounds of the $MeLn_4Mo_3O_{15}F$ (*Me* = Li, Na; *Ln* = La–Nd) composition were obtained. Such cation–anion

doping of $Ln_5Mo_3O_{16+\delta}$ phases leads to the appearance of a reversible phase transition in these materials, accompanied by a jump in conductivity by several orders of magnitude.

The explanation of a noticeable change in the physical properties during fluorination of Hubert phases is impossible without an accurate description of the crystal structure of the compounds. In this work, we carried out an accurate X-ray diffraction analysis of $LiLa_4Mo_3O_{15}F$ single crystals at 20 and −183 °C.

2. Materials and Methods

Polycrystalline samples of nominal composition $LiLa_4Mo_3O_{15}F$ were obtained by solid-phase synthesis in air from a stoichiometric mixture of LiF, La_2O_3, and MoO_3 (99.9%) reagents using two-stage firing at temperatures of 600 and 700 °C for 12 h. The heating and cooling rate was 5 °C min^{-1}.

The main problem of growing $LiLa_4Mo_3O_{15}F$ single crystals is the intense evaporation of fluorine above 700–800 °C [16], which requires the selection of a special low-melting solvent. Single crystals of $Li_xLa_{5-x}Mo_3O_{16.5-y}F_y$ were grown by flux method (according to [16], the actual content of lithium and fluorine in crystals may differ from the nominal composition of $LiLa_4Mo_3O_{15}F$). When preparing the solvent, we focused on the binary system 60 mol% Li_2MoO_4–40 mol% LiF. To obtain the Li_2MoO_4 compound and maintain the indicated proportion, we took 60 mol% Li_2CO_3 and 60 mol% MoO_3. Thus, a mixture of reagents Li_2CO_3 (60 mol%), MoO_3 (60 mol%), and LiF (40 mol%) was used as a solvent. The main advantage of this solvent is its low melting point (650 °C), which makes it possible to avoid intense evaporation of fluorine, which was observed for $LiLa_4Mo_3O_{15}F$ above 700–800 °C [16].

Preliminarily prepared polycrystalline samples of $LiLa_4Mo_3O_{15}F$ with a total weight of about 4 g were placed on the bottom of a platinum crucible (25 mL); then, the crucible with ceramics was filled with a solvent mixture (40 g) and placed in an oven, where it was heated to 720 °C. At this temperature, the solvent melted and became transparent, and the ceramic partially dissolved in it. A certain amount of ceramic material remained at the bottom of the crucible and acted as a seed. An increase in the melt temperature led to the appearance of numerous bubbles on the ceramic surface, indicating the evaporation of fluorine.

The melt was kept at 720 °C for seven days. Then, the melt was slowly cooled at a rate of 1 °C h^{-1} to a temperature of 650 °C, at which its complete solidification was observed. After that, the crucible was cooled to room temperature at a rate of 50 °C h^{-1}. The crystals were easily washed from the solvent with hot water.

Differential scanning calorimetry (DSC) of single crystals was carried out on a NETZSCH STA 449C instrument (Selb, Germany) in Al_2O_3 crucibles in air. The rate of heating and cooling of the samples was 10 °C min^{-1}.

The concentration of lithium ions in $LiLa_4Mo_3O_{15}F$ single crystals was measured using an iCapQc mass spectrometer (Thermo Fischer Scientific, Bremen, Germany) with ionization in inductively coupled plasma (ICP-MS technique). Single crystals of $Li_xLa_{5-x}Mo_3O_{16.5-y}F_y$ phase with a total weight of 0.03 g were selected for the study. The decomposition of single crystals was carried out in a mixture of concentrated acids, H_2SO_4 (2 mL) and H_3PO_4 (2 mL), in a microwave autoclave in a fluoroplastic container at a temperature of 240 °C for 1.5 h; the settling time was 55 min. The resulting solution was diluted in two stages. First, 6 mL of deionized water with a residual resistance of 18.2 MOhm was added, bringing the total volume of the solution to 10 mL. Then, 1 mL of the resulting solution was diluted 50 times with deionized water and 2% of HNO_3 was added. This solution was examined on a spectrometer. The final concentration of the matrix in the test solution was 0.1 g/L. The measurements were carried out three times to achieve convergence of the results. Nitric (HNO_3 65%, EMSURE ISO, Merck, Darmstadt, Germany), sulfuric (H_2SO_4 98%, EMSURE ISO, Merck, Darmstadt, Germany), and phosphorus (H_3PO_4 98%, ACROS, Geel, Belgium) acids of appropriate purity were used during sample preparation as well as a CEM Mars 6 microwave decomposition system. Calibration was carried out using a standard MS-68A

multi-element solution. An aliquot of the Sc solution (2 ppb) was used to control the sensitivity to the matrix effect. Calibration, elemental analysis, and corrections for spectral overlap were performed using the QTegraThermoFisher program.

Powder X-ray phase analysis was performed at room temperature on a Rigaku Miniflex 600 diffractometer (CuK_α radiation, 2θ = 10°–70°, 0.02° scan step). The synthesis products were carefully ground to a finely dispersed state in an agate mortar and placed in an X-ray amorphous quartz cuvette with the addition of alcohol. The experimental data obtained were processed using the Miniflex Guidance, PDXL-2, Match software package and the current ICDD PDF-2 and ICSD databases. Quantitative analysis by the Rietveld method was carried out using the JANA2006 program [18]. The refinement of the phase relationships was carried out by stepwise adding the refined parameters from the most stable to the correlating ones, with constant graphical modeling of the background until the values of the *R*-factors stabilized.

The intensities of diffraction reflections from $Li_xLa_{5-x}Mo_3O_{16.5-y}F_y$ single crystals no larger than 0.3 mm in size were measured at 20 and −183 °C on an XtaLAB Synergy-DW (MoK_α) X-ray diffractometer (Rigaku Oxford Diffraction). The CrysAlisPro program [19] was used for experimental data reduction. Absorption correction was made taking into account the shape and sizes of the samples using a Gaussian grid and numerical integration [18]. The JANA2006 software package was used to refine the structural model. The coordinates of lanthanum, molybdenum, and oxygen atoms were found by the charge-flipping method using the Superflip program [20]. Lithium and fluorine atoms were localized from difference Fourier maps of electron density, calculated, and analyzed at the final stage of refinement of the structural parameters of lanthanum, molybdenum, and oxygen atoms. The structural data are deposited with the Cambridge Crystallographic Data Centre. CCDC references: 2257767; 2257768.

3. Results and Discussion

3.1. Powder X-ray Diffraction and Elemental Analysis

Dark yellow cubic crystals of $Li_xLa_{5-x}Mo_3O_{16.5-1.5y}F_y$ were obtained as the main phase and white plate-like LiF crystals as the second phase. A photograph of cubic $Li_xLa_{5-x}Mo_3O_{16.5-1.5y}F_y$ single crystals as well as their diffraction pattern are shown in Figure 1. The size of the obtained single crystals was 0.2–0.3 mm.

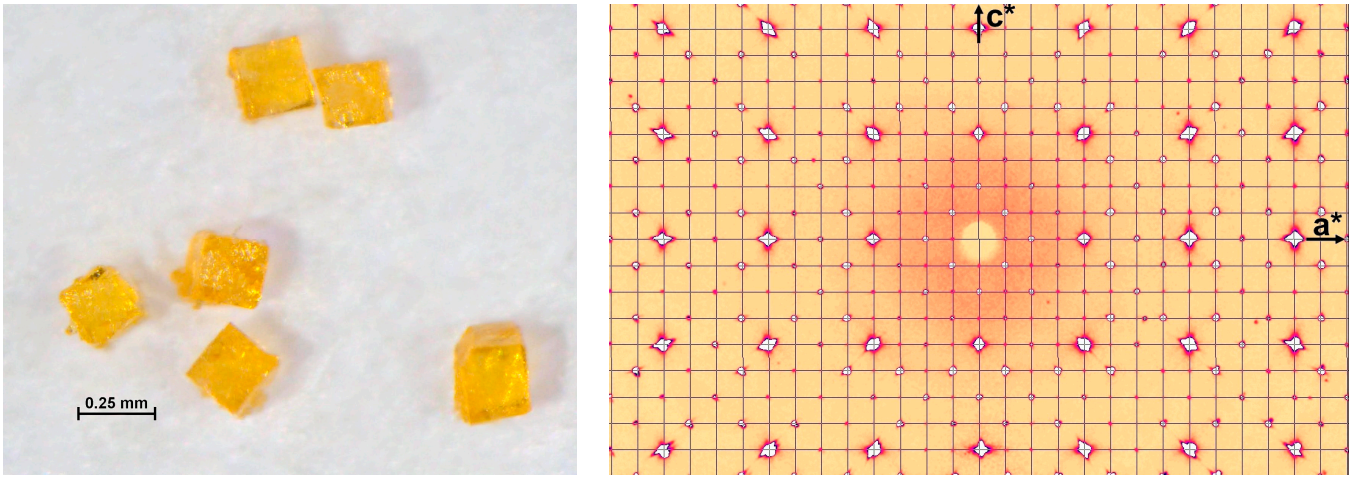

(**a**) (**b**)

Figure 1. $Li_xLa_{5-x}Mo_3O_{16.5-y}F_y$ single crystals: (**a**) Photograph of crystals illuminated with an LED lamp (5600 K); (**b**) X-ray diffraction pattern in the (*h*0*l*) plane at 90 K.

According to the X-ray diffraction pattern obtained from the grown crystal mixture (Figure 2), the main synthesized phase is a cubic fluorite-like compound isostructural to the cubic $Ln_5Mo_3O_{16}$ (Ln = La–Gd) molybdate family [1,5,7]. The reflections fixed at 2θ = 38.85°, 45.14°, and 65.6° refer to lithium fluoride crystals synthesized as the second phase [21]. The unit cell parameter a for $Li_xLa_{5-x}Mo_3O_{16.5-y}F_y$ single crystals is 11.249(4) Å, which is in good agreement with the data in Table 1 (see below) as well as with the unit cell parameter of ceramics of the same composition obtained in [16]. In addition to the main phase and LiF phase, the synthesis product contained a small amount of the $LiLa(MoO_4)_4$ phase. We carried out a full profile analysis. Unfortunately, it was not possible to determine the concentration of the $LiLa(MoO_4)_4$ phase due to the small number of low-intensity peaks in the diffraction pattern. The total values of the R-factors of the diffraction profile obtained at the final stage of the analysis were S_p = 1.91 (S is goodness of fit), R_p = 12.37%, and R_{pw} = 16.41%. The R-factors were R = 5.07%, R_w = 5.60% for the detected main phase and R = 9.59%, R_w = 11.58% for the LiF phase. The concentrations of the main phase and LiF are 38(1) and 62(1) wt%, respectively.

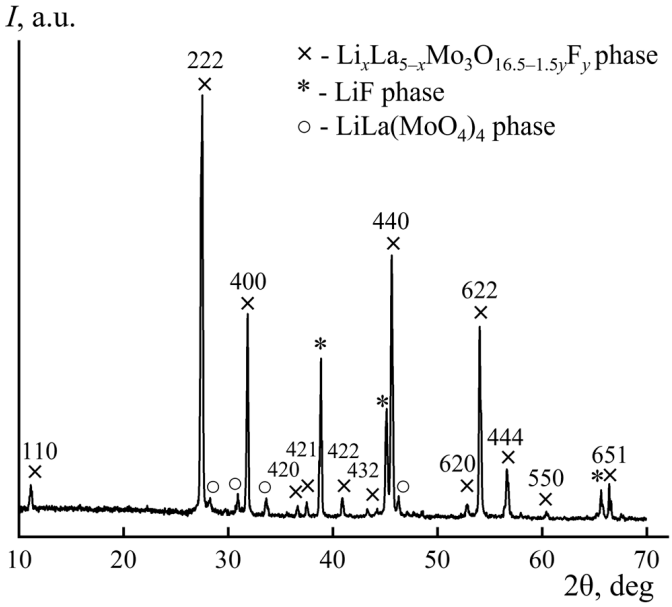

Figure 2. Powder X-ray diffraction patterns of crystal mixture obtained in the experiment on growing single crystals.

To obtain data on the quantitative lithium content in $Li_xLa_{5-x}Mo_3O_{16.5-y}F_y$ single crystals, the ICP-MS technique was used. ICP-MS analysis confirmed the presence of lithium cations in the solution in the amount of 2591.17 μg per 1 g of sample (0.259 wt%). According to the measured concentration, the chemical formula of the $La_{4.55}Li_{0.45}Mo_3O_{16.5-y}F_y$ compound was calculated, which is consistent with X-ray analysis data ($La_{4.58}Li_{0.42}Mo_3O_{15.76\pm\delta}F_{0.42\pm\varepsilon}$) (Table 1).

Figure 3 shows DSC data for $Li_xLa_{5-x}Mo_3O_{16.5-y}F_y$ single crystals upon heating and cooling in air. The DSC curve demonstrates a reversible peak at 574 °C (heating) and 529 °C (cooling), which corresponds to a reversible first-order phase transition. A similar reversible phase transition, accompanied by a sharp jump in conductivity, was observed for F-containing ceramics $MLn_4Mo_3O_{16.5-x}F_x$ (M = Li, Na) [15,16]. It is important to note that no phase transitions are detected in samples of the $Ln_5Mo_3O_{16+\delta}$ family that do not contain fluorine. Therefore, the presence of such a phase transition can be considered as indirect evidence of the presence of fluorine in the structure of the compound.

Table 1. Crystallographic characteristics, experimental data, and the results of structure refinement for $Li_xLa_{5-x}Mo_3O_{16.5-y}F_y$ single crystals.

Chemical formula	$Li_{0.42}La_{4.58}Mo_3O_{15.76\pm\delta}F_{0.42\pm\varepsilon}$	$Li_{0.42}La_{4.58}Mo_3O_{15.76+\delta}F_{0.42\pm\varepsilon}$
Space group, Z	$Pn\bar{3}n$, 4	$Pn\bar{3}n$, 4
T, °C	20	−183
a, Å	11.2706(1)	11.2501(1)
V, Å^3	1431.66(1)	1423.87(1)
D, g/cm^3	5.506	5.536
Radiation; λ, Å	Mo K_α; 0.71073	Mo K_α; 0.71073
μ, mm^{-1}	15.964	16.051
Sample size, mm	0.233 × 0.178 × 0.172	0.233 × 0.178 × 0.172
Diffractometer	Rigaku XtaLAB Synergy-DW, HyPix-Arc 150	Rigaku XtaLAB Synergy-DW, HyPix-Arc 150
Scan mode	ω	ω
Absorption correction; T_{min}, T_{max},	Gaussian; 0.092, 0.275,	Gaussian; 0.138, 1.000,
θ_{max}, deg	59.71	59.89
Ranges of indices h, k, l	$-25 \le h \le 25$, $-27 \le k \le 27$, $-27 \le l \le 27$	$-27 \le h \le 27$, $-27 \le k \le 27$, $-25 \le l \le 25$
Number of reflections: measured/unique, $R_{int}/I > 3\sigma(I)$	1220187/1820, 0.06/580	822160/1090, 0.11/559
Refinement method	Least-squares method based on F	Least-squares method based on F
Number of parameters	23	23
$R(\lvert F \rvert)/wR(\lvert F \rvert)$	0.0143/0.0257	0.0159/0.0248
S	2.37	2.24
$\Delta\rho_{min}/\Delta\rho_{max}$	−0.80/1.05	−0.99/1.27
Programs	CrysAlis [19], JANA2006 [18]	CrysAlis [19], JANA2006 [18]

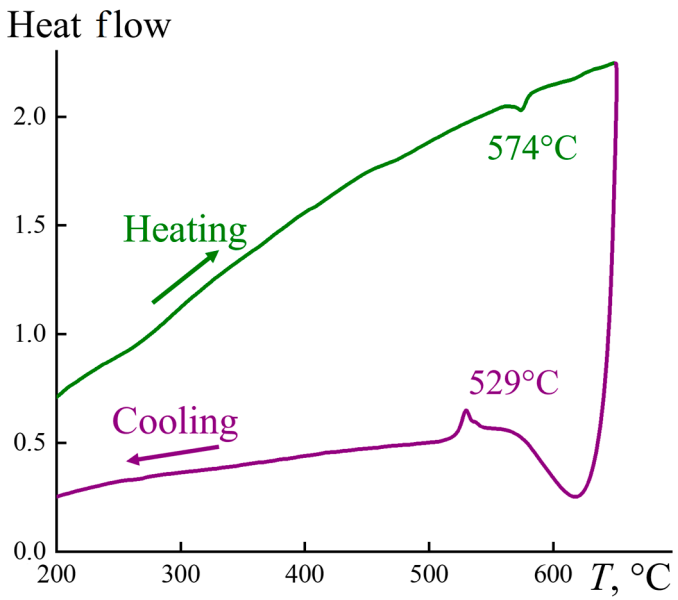

Figure 3. DSC data for $Li_xLa_{5-x}Mo_3O_{16.5-y}F_y$ single crystals upon heating and cooling in air.

3.2. Crystal Structure

Experimental data, the main crystallographic parameters, and the results of structure refinement of $Li_xLa_{5-x}Mo_3O_{16.5-y}F_y$ single crystals are listed in Table 1.

The structure of $Li_xLa_{5-x}Mo_3O_{16.5-y}F_y$ single crystals was studied by X-ray diffraction analysis at 20 and −183 °C. The compound has a cubic structure (space group $Pn\bar{3}n$), which is consistent with the literature data [6,7]. No structural phase transition was revealed with decreasing temperature. The search for a unit cell in the studied single crystal ended with the choice of a cubic cell with parameter a = 11.2706(1) Å at room temperature, which made it possible to index more than 96% of the measured reflections, and a = 11.2501(1) Å at −183 °C, which made it possible to index more than 93% of the measured reflections. The obtained unit cell parameters correlate with the unit cell parameter of fluorite CaF_2 as $a \approx 2a_f$ (a_f = 5.5 Å). The unit cell of the lattice of the cubic modification of the $Li_xLa_{5-x}Mo_3O_{16.5-y}F_y$ single crystal contains six independent atoms: two La atoms, one Mo atom, and two O atoms, located in the main crystallographic positions, and one O atom in the interstice. At the stage of refining the coordinates and atomic displacement parameters in the anisotropic approximation for La1 (Wyckoff position 12*e*), La2 (8*c*), Mo (12*d*), O1 (16*f*), and O2 (48*i*) atoms and in the isotropic approximation for O3 (2*a*) atoms, the values of the occupancies of La1, La2, and Mo atoms of their crystallographic positions were refined and vacancies in the positions of the La2 atom were revealed. It was assumed that these positions were occupied statistically by the atoms of lanthanum and lithium. The occupancies of the La2/Li2 mixed positions were refined under the assumption that they were fully occupied. The following values of position occupancy by lanthanum and lithium atoms in the structure were obtained: 78.8(2)% for La2 and 21.2% for Li2. It is noteworthy that the impurity (lithium) atoms do not enter the position of the La1 atom, which is consistent with the data obtained earlier for the $Ln_5Mo_3O_{16.5}$ compounds doped with lead atoms [9] or calcium [10]. Thus, regardless of the size of the impurity cation in the structure of the $Ln_5Mo_3O_{16.5}$ compound, it substitutes for the rare-earth element only in the second of two *Ln* crystallographic positions. This may be because, in the $Ln_5Mo_3O_{16.5}$ structure, the *Ln*1 atom is surrounded by four O1 atoms at a distance of 2.432(1) Å and four O2 atoms at a distance of 2.652(1) Å, and the *Ln*2 atom is surrounded by two O1 atoms at a distance of 2.272(1) Å and six O2 atoms at a distance of 2.693(1) Å. Therefore, the coordination polyhedron of the *Ln*2 atom is much more distorted than the coordination polyhedron of the *Ln*1 atom. It should be noted that the interstitial oxygen O3 atom is located at 2.681(3) Å from the *Ln*1 atom. The chemical formula of the studied single crystal $Li_{0.423}La_{4.577}Mo_3O_{16.5-y}F_y$ was obtained from the values of the occupancies of the crystallographic positions by cations in the structure. For the electrical neutrality of the chemical formula, some of the O3 atoms were replaced by fluorine atoms (Figures 4 and 5). It should also be noted that the O2 crystallographic position is not fully occupied (qO2 = 0.97(2)). The final chemical formula of the studied single crystals is $Li_{0.42}La_{4.58}Mo_3O_{15.76\pm\delta}F_{0.42\pm\varepsilon}$.

A partial substitution of fluorine anions for oxygen atoms in the interstices makes it possible to explain the change in the physical properties of fluorinated molybdates in terms of bond characteristics such as polarizability and the degree of ionicity of the metal–oxygen bond. The difference in electronegativity for La–F (Δ = 2.88) or Li–F (Δ = 3) according to Pauling increases compared to metal–oxygen bonds La–O (Δ = 2.34) or Li–O (Δ = 2.46), making them more ionic and, consequently, less strong. One of the main factors determining the mobility of ionic carriers in solids is the change in the degree of ionicity of the metal–oxygen bond. In addition, the appearance of anions of a different nature (O^{2-} and F^-) in the oxygen sublattice in low concentrations can lead to the effects of additional electrostatic repulsion between these anions and, consequently, to an increase in oxygen mobility, which increases oxygen conductivity. A similar effect was also observed in [22], where the effect of doping with fluorine on the transport properties (oxygen-ion and proton conductivity) of complex oxides of the perovskite family was studied.

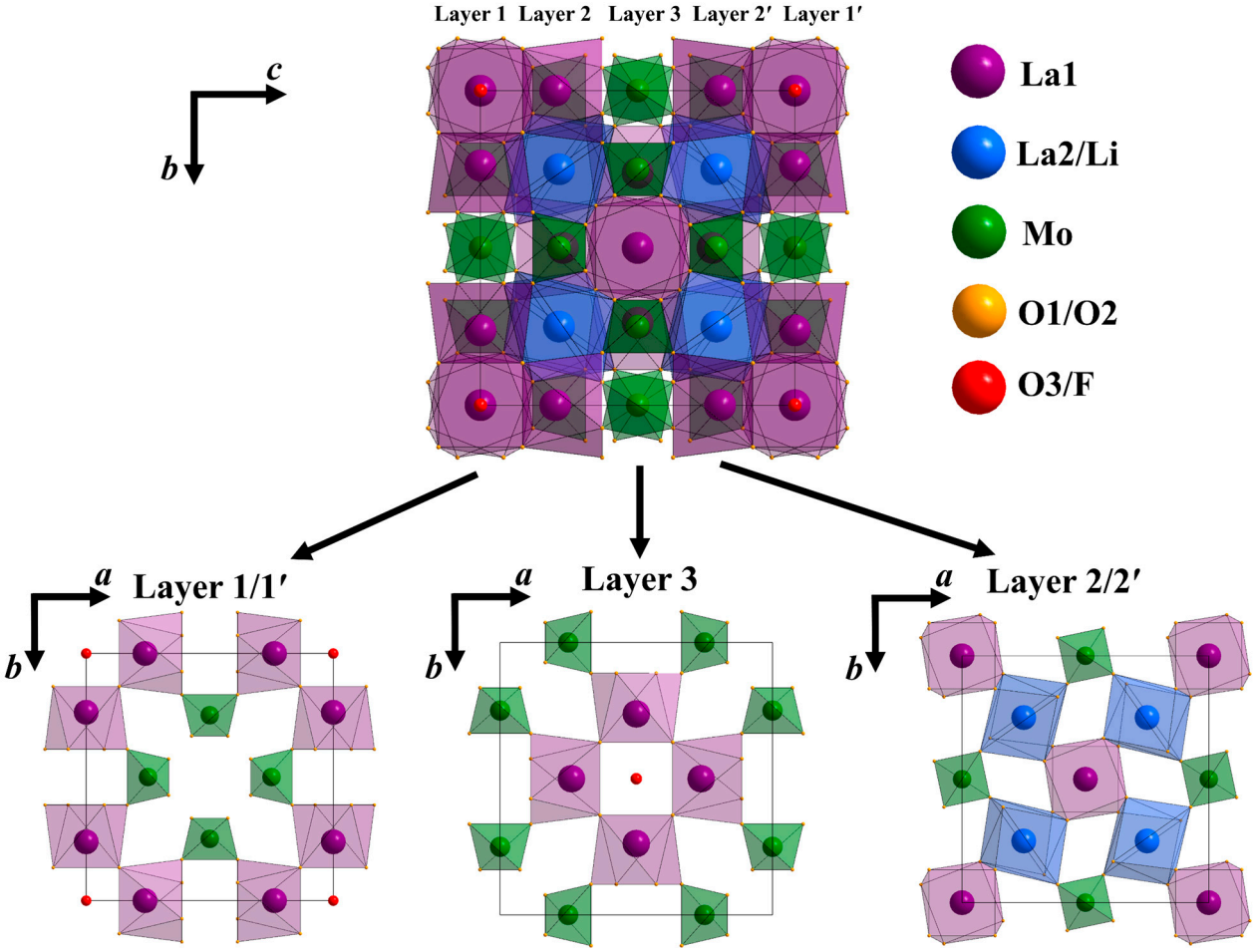

Figure 4. Layered image of the model of the crystal structure of the compound $Li_{0.42}La_{4.58}Mo_3O_{15.76\pm\delta}F_{0.42\pm\varepsilon}$. In layers 1 and 1′, the La1 atoms are bound by translation along the *c* axis, symmetry operation $x, y, 1 + z$. In layers 2 and 2′, the La2 atoms are bound by the symmetry operation $x, z, 1 - y$.

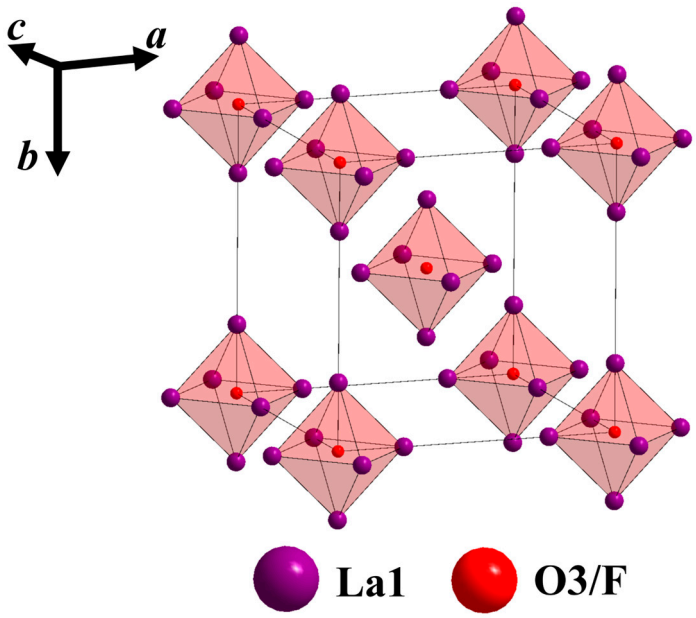

Figure 5. Cation environment of O3/F positions in the $Li_{0.42}La_{4.58}Mo_3O_{15.76\pm\delta}F_{0.42\pm\varepsilon}$ structure.

4. Conclusions

Fluorine-containing rare-earth molybdates of the $Li_{0.423}La_{4.577}Mo_3O_{15.76\pm\delta}F_{0.424\pm\varepsilon}$ composition from the $Ln_5Mo_3O_{16+\delta}$ oxygen–electron conductor family were obtained for the first time as single crystals by the flux method. The accurate X-ray diffraction analysis confirmed that the crystals obtained are isostructural to the fluorine-free analogue with a cubic structure (space group $Pn\bar{3}n$). Lithium atoms replace one of the two positions of lanthanum, preferring a more distorted LaO_8 polyhedron. Fluorine atoms replace the positions of over-stoichiometric oxygen located in the vast cavities of the structure. The increase in the degree of ionicity of the metal–oxygen bond and additional electrostatic repulsion of two different anions can affect the transport characteristics of the material, increasing the conductivity of the compounds with partial substitution of fluorine anions for oxygen atoms.

Author Contributions: Synthesis of polycrystalline samples, single crystals growth by the flux method, writing the article, original draft preparation, E.I.O.; X-ray phase analysis, T.A.S.; ICP-MS analysis, V.B.K.; X-ray diffraction analysis, visualization, A.M.A.; X-ray diffraction analysis, visualization, translation, data curation, N.E.N.; single crystal growth by the flux method, DSC analysis, E.P.K.; X-ray diffraction analysis, writing the article, original draft preparation, supervision, N.I.S.; writing the article, original draft preparation, reviewing and editing, project administration, O.A.A.; project administration, V.I.V. All authors have read and agreed to the published version of the manuscript.

Funding: This research was funded by the Russian Science Foundation, grant number 23-12-00221.

Data Availability Statement: Cambridge Crystallographic Data Centre. CCDC references: 2257767; 2257768.

Acknowledgments: This work was performed using the equipment of the Shared Research Center FSRC "Crystallography and Photonics" RAS.

Conflicts of Interest: The authors declare no conflict of interest.

References

1. Hubert, P.H.; Michel, P.; Thozet, A. Structure du molybdate de néodyme $Nd_5Mo_3O_{16}$. *C. R. Hebd. Seances Acad. Sci. Ser. C* **1973**, *276*, 1779–1781.
2. Istomin, S.Y.; Kotova, A.I.; Lyskov, N.V.; Mazo, G.N.; Antipov, E.V. $Pr_5Mo_3O_{16+\delta}$: A new anode material for solid oxide fuel cells. *Russ. J. Inorg. Chem.* **2018**, *63*, 1274–1279. [CrossRef]
3. Tsai, M.; Greenblatt, M. Oxide ion conductivity in $Ln_5Mo_3O_{16+x}$ (*Ln* = La, Pr, Nd, Sm, Gd; *x*~0.5) with a fluorite-related structure. *Chem. Mater.* **1989**, *1*, 253–259. [CrossRef]
4. Voronkova, V.I.; Leonidov, I.A.; Kharitonova, E.P.; Belov, D.A.; Patrakeev, M.V.; Leonidova, O.N.; Kozhevnikov, V.L. Oxygen ion and electron conductivity in fluorite-like molybdates $Nd_5Mo_3O_{16}$ and $Pr_5Mo_3O_{16}$. *J. Alloys Compd.* **2014**, *615*, 395–400. [CrossRef]
5. Biendicho, J.J.; Playford, H.Y.; Rahman, S.M.H.; Norberg, S.T.; Eriksson, S.G.; Hull, S. The fluorite-like phase $Nd_5Mo_3O_{16\pm\delta}$ in the MoO_3–Nd_2O_3 system: Synthesis, crystal structure, and conducting properties. *Inorg. Chem.* **2018**, *57*, 7025–7035. [CrossRef] [PubMed]
6. Martinez-Lope, M.J.; Alonso, J.A.; Sheptyakov, D.; Pomyakushin, V. Preparation and structural study from neutron diffraction data of $Pr_5Mo_3O_{16}$. *J. Solid State Chem.* **2010**, *183*, 2974–2978. [CrossRef]
7. Alekseeva, O.A.; Gagor, A.B.; Pietraszko, A.P.; Sorokina, N.I.; Bolotina, N.B.; Artemov, V.V.; Kharitonova, E.P.; Voronkova, V.I. Crystal structure of the oxygen conducting compound $Nd_5Mo_3O_{16}$. *Z. Kristallogr.* **2012**, *227*, 869–875. [CrossRef]
8. Faurie, J.-P. Préparation de nouvelles phases $MLn_4Mo_3O_{16}$, $MLn_6Mo_4O_{22}$ de structure dérivée du type fluorine. *Bull. Soc. Chim. Fr.* **1971**, *11*, 3865–3868.
9. Antipin, A.M.; Sorokina, N.I.; Alekseeva, O.A.; Kharitonova, E.P.; Orlova, E.I.; Voronkova, V.I. Crystal structure of fluorite-like compound based on $Nd_5Mo_3O_{16}$ with lead partly substituting for neodymium. *Acta Crystallogr.* **2015**, *B71*, 186–193. [CrossRef]
10. Voronkova, V.I.; Kharitonova, E.P.; Orlova, E.I.; Levchenko, A.V.; Antipin, A.M.; Sorokina, N.I.; Belov, D.A. Ca-doped fluorite-like compounds based on $Nd_5Mo_3O_{16}$. *J. Alloys Compd.* **2016**, *673*, 314–320. [CrossRef]
11. Vu, T.D.; Krichen, F.; Barre, M.; Busselez, R.; Adil, K.; Jouanneaux, A.; Suard, E.; Goutenoire, F. Crystal structure and ion conducting properties of $La_5NbMo_2O_{16}$. *J. Solid State Chem.* **2016**, *237*, 411–416. [CrossRef]
12. Antipin, A.M.; Sorokina, N.I.; Alekseeva, O.A.; Zubavichus, Y.V.; Artemov, V.V.; Kharitonova, E.P.; Orlova, E.I.; Voronkova, V.I. Structure of $Nd_5Mo_3O_{1+\delta}$ single crystals doped with tungsten. *Crystallogr. Rep.* **2018**, *63*, 339–343. [CrossRef]
13. Antipin, A.M.; Alekseeva, O.A.; Sorokina, N.I.; Verin, I.A.; Novikova, N.E.; Furmanova, N.G.; Kharitonova, E.P.; Voronkova, V.I. Single-crystal structure of vanadium-doped $Nd_5Mo_3O_{16}$. *Crystallogr. Rep.* **2014**, *59*, 141–145. [CrossRef]

14. Voronkova, V.I.; Kharitonova, E.P.; Orlova, E.I. Synthesis and electrical properties of a fluorite-Like $Nd_5Mo_3O_{16}$ compound with partial substitution of molybdenum by tungsten, niobium, or vanadium. *Crystallogr. Rep.* **2018**, *63*, 127–131. [CrossRef]
15. Voronkova, V.; Kharitonova, E.; Orlova, E.; Kezionis, A.; Petrulionis, D. Effect of sodium and fluorine co-doping on the properties of fluorite-like rare-earth molybdates of $Nd_5Mo_3O_{16}$ type. *Eur. J. Inorg. Chem.* **2019**, *9*, 1250–1256. [CrossRef]
16. Voronkova, V.; Kharitonova, E.; Orlova, E.; Baldin, E.; Gorshkov, N.; Goffman, V.; Chernyak, S. Fluorite-like $Li_xLn_{5-x}Mo_3O_{16.5-1.5x}F_x$ (*Ln* = La, Pr, Nd) compounds isostructural with $Nd_5Mo_3O_{16}$. *J. Am. Ceram. Soc.* **2020**, *103*, 6414–6423. [CrossRef]
17. Baldin, E.D.; Sorokin, T.A.; Orlova, E.I.; Gorshkov, N.V.; Kharitonova, E.P.; Lyskov, N.V.; Goffman, V.G.; Voronkova, V.I. Proton conductivity in rare-earth fluorine-containing molybdates $NaLn_4Mo_3O_{15}F$. *Russ. J. Electrochem.* **2023**, *59*, 54–59. [CrossRef]
18. Petříček, V.; Dušek, M.; Palatinus, L. Crystallographic computing system JANA2006: General features. *Z. Kristallogr.* **2014**, *229*, 345–352. [CrossRef]
19. Rigaku Oxford Diffraction. *CrysAlisPro Software System, Version 42.74a*; Rigaku Corporation: Oxford, UK, 2018.
20. Palatinus, L. Ab initio determination of incommensurately modulated structures by charge flipping in superspace. *Acta Crystallogr. A* **2004**, *60*, 604–610. [CrossRef]
21. Swanson, H.E.; Tatge, E. Standard X-ray diffraction powder patterns. *Natl. Bur. Stand. (U.S.) Circ.* **1953**, *539*, 1.
22. Tarasova, N.A. Effect of fluorine doping on the ionic (O^{2-}, H^+) conductivity of oxygen-deficient complex oxides. *Russ. Chem. Bull.* **2020**, *69*, 1253–1263. [CrossRef]

Disclaimer/Publisher's Note: The statements, opinions and data contained in all publications are solely those of the individual author(s) and contributor(s) and not of MDPI and/or the editor(s). MDPI and/or the editor(s) disclaim responsibility for any injury to people or property resulting from any ideas, methods, instructions or products referred to in the content.